Molecular Genetics and Metabolism Reports 6 (2016) 48–54

Contents lists available at ScienceDirect

Molecular Genetics and Metabolism Reports

journal homepage: www.elsevier.com/locate/ymgmr

# Preferred transduction with AAV8 and AAV9 via thalamic administration in the MPS IIIB model: A comparison of four rAAV serotypes

J.A. Gilkes , M.D. Bloom, C.D. Heldermon *

*Department of Medicine, University of Florida, Gainesville, FL, USA*

ARTICLE INFO

*Article history:*
Received 9 November 2015
Received in revised form 30 November 2015
Accepted 30 November 2015
Available online 7 December 2015

*Keywords:*
MPS IIIB
Mucopolysaccharidosis type III B
Gene therapy
Adeno-associated virus
AAV
Lysosomal storage disease

ABSTRACT

Sanfilippo syndrome type B (MPS IIIB) is a lysosomal storage disease caused by a deficiency of N-acetyl-glucosaminidase (NAGLU) activity. Since early therapeutic intervention is likely to yield the most efficacious results, we sought to determine the possible therapeutic utility of rAAV in early gene therapy based interventions. Currently, the application of recombinant adeno-associated virus (AAV) vectors is one of the most widely used gene transfer systems, and represents a promising approach in the treatment of MPS IIIB. From a translational standpoint, a minimally invasive, yet highly efficient method of vector administration is ideal. The thalamus is thought to be the switchboard for signal relay in the central nervous system (CNS) and therefore represents an attractive target. To identify an optimal AAV vector for early therapeutic intervention, and establish whether thalamic administration represents a feasible therapeutic approach, we performed a comprehensive assessment of transduction and biodistribution profiles of four green fluorescent protein (GFP) bearing rAAV serotypes, -5, -8, -9 and -rh10, administered bilaterally into the thalamus. Of the four serotypes compared, AAV8 and -9 proved superior to AAV5 and -rh10 both in biodistribution and transduction efficiency profiles. Genotype differences in transduction efficiency and biodistribution patterns were also observed. Importantly, we conclude that AAV8 and to a lesser extent, AAV9 represent preferable candidates for early gene therapy based intervention in the treatment of MPS IIIB. We also highlight the feasibility of thalamic rAAV administration, and conclude that this method results in moderate rAAV biodistribution with limited treatment capacity, thus suggesting a need for alternate methods of vector delivery.



## 1. Introduction

A deficiency in N-acetyl-glucosaminidase activity results in the lysosomal storage disease, mucopolysaccharidosis IIIB (MPS IIIB), commonly referred to as Sanfilippo syndrome type B. Although heterogeneous in clinical presentation, this disease typically manifests around 5 years of age. Over time, progressive mental degeneration results in severe impairment of neurocognitive ability and loss of motor function. Death often occurs between the ages of 15–20 years [1,2]. There is currently no cure for MPS IIIB. The well characterized MPS IIIB mouse model possesses many of the same biochemical, histological and clinical features as the human disease, and is therefore utilized in studies to evaluate therapeutic candidates [3,4].

The recombinant adeno-associated virus (rAAV) vector gene transfer system has emerged as a powerful tool for therapeutic gene delivery and is favored over other viral vectors due to its low immunogenicity, ability to transduce both dividing and non-dividing cells, long lasting gene expression, non-pathogenicity, and importantly, clinical safety [5–7]. The most commonly used AAV vectors are based on AAV serotype 2. Several AAV serotypes allow cross-packaging of the AAV2 vector backbone [8–10]. Since AAV transduction is modulated by the presence and distribution of cell surface receptors, differential cellular tropism and transduction efficiency has been observed [11,12]. This phenomenon is also suggested to occur in an age dependent manner [13–15]. Studies suggest that the greatest therapeutic outcome would stem from early treatment intervention, before disease pathology becomes evident and irreversible [14,16]. It is possible that rAAV efficiency may be differentially modulated depending on the disease model and associated extracellular mileau.

Widespread gene delivery throughout the central nervous system (CNS) remains a major challenge to successful treatment due to the need to overcome the blood brain barrier (BBB). To circumvent this limitation, direct CNS administration of rAAVs is typically performed. We have previously demonstrated improvement in behavioral measures,

*Abbreviations:* rAAV, recombinant adeno-associated virus; ANOVA, analysis of variance; MPS IIIB, mucopolysaccharidosis type III B; CNS, central nervous system; BBB, blood brain barrier; NeuN, neuronal nuclear protein; GFAP, glial fibrillary acidic protein; hGFP, humanized green fluorescent protein.

* Corresponding author at: 1600 SW Archer Rd, Campus Box 100277, Gainesville, FL 32608, USA.
*E-mail address:* coy.heldermon@medicine.ufl.edu (C.D. Heldermon).

http://dx.doi.org/10.1016/j.ymgmr.2015.11.006

lysosomal storage and lifespan of MPS IIIB mice with intracranial delivery of AAV5 pseudotyped vector to the CNS [17] but this treatment did not completely correct the disease. To this end, our goal is to assess several CNS trophic rAAV serotypes in the MPS IIIB neonatal mouse brain to determine which rAAV serotype facilitates the best transduction and biodistribution profiles. To limit the invasiveness of the procedure, we assess the methodological utility of a one-time delivery of rAAV vector bilaterally into the thalamus. We anticipate that these results will contribute to clinical approaches in determining the optimal gene delivery vector and method of delivery for age dependent treatment of MPS IIIB.

## 2. Results

### *2.1. Differential biodistribution profiles observed for different AAV serotypes*

The thalamus is considered an information hub, with complex networks of connections within the brain (Fig. 1A). To facilitate vector biodistribution, we sought to exploit these thalamic connections. Control and MPS IIIB mice received bilateral intracranial administration of GFP-AAV5, -8, -9 and -rh10 into the thalamus. Evans Blue dye was injected to visualize predicted spread and biodistribution of vectors after administration (Fig. 1B). We initially sought to determine the biodistribution profiles of the different serotypes. Three months after vector administration, brain tissue of euthanized animals was analyzed to determine the presence and location of GFP. Moderate expression of GFP was observed in the cortex, thalamus and hippocampus of animals treated with AAV8 and -9. AAVrh10 treated animals showed minimal GFP staining in the cortex, with some presence in the hippocampus. AAV5 yielded the least favorable results as GFP expression was minimally seen in any of the analyzed regions (Fig. 1C). Furthermore, we noted that the thalamic method of administration does not readily facilitate vector spread into the cerebellum by any serotype. The retardation of motor function is a severe impediment suffered by MPS IIIB patients. The regulation of motor coordination is an important function of the cerebellum, therefore making it an important structural area to target in order to achieve maximal therapeutic success.

Next, we performed a qualitative assessment of GFP–AAV biodistribution profiles based on serotype (Fig. 2A) and quantified GFP expression in distinct structurally and functionally relevant areas in mid-sagittal brain sections (Fig. 2B). Comparative qualitative assessment of GFP expression patterns revealed that AAV5–GFP expression was heavily localized with ependymal cells, and otherwise exhibited minimal punctate distribution in the cortex (Fig. 2A, *inset*). In MPS IIIB treated animals, thalamic administration of AAV8 vector resulted in appreciable spread of vector into the somatosensory and visual areas of the cortex. Layers II/III of the cortex exhibited light GFP expression, while layers IV and V exhibited moderate to heavy GFP expression. Ventral spread of the AAV8–GFP vector was observed in the hippocampus and proximal areas of thalamus closest to the hippocampus and often along the thalamocortical or fiber tracks surrounding the thalamus. In the hippocampus, moderate staining was witnessed in CA1, CA2 and CA3 regions. Control animals in the AAV8 treated group exhibited a different transduction profile compared to MPS IIIB treated animals, with localized cortical spread and minimal thalamic penetration. This data suggests that there may be an interplay of unknown factors modulating transduction between these two genotypes. Both genotypes in the AAV9 treated groups showed comparable biodistribution profiles. AAVrh10 distribution comparisons were difficult due to low overall expression, although it was primarily localized to the thalamus (Fig. 2A). Quantitative assessment of AAV–GFP biodistribution into the cortex, hippocampus, thalamus and cerebellum revealed that in the Control group, AAV8 and -9 were superior to AAV5 and -rh10 in the cortex ($p < 0.05$ vs -5 and -rh10) and hippocampus (AAV8 vs -5 and -rh10, $p < 0.001$), but not thalamus and cerebellum. Whereas, in the MPS IIIB treated group, the largest GFP positive areas were the cortex with approximately 3% total area, and this was accomplished by AAV8, and to a lesser degree, AAV9. In the cortex, AAV8 was

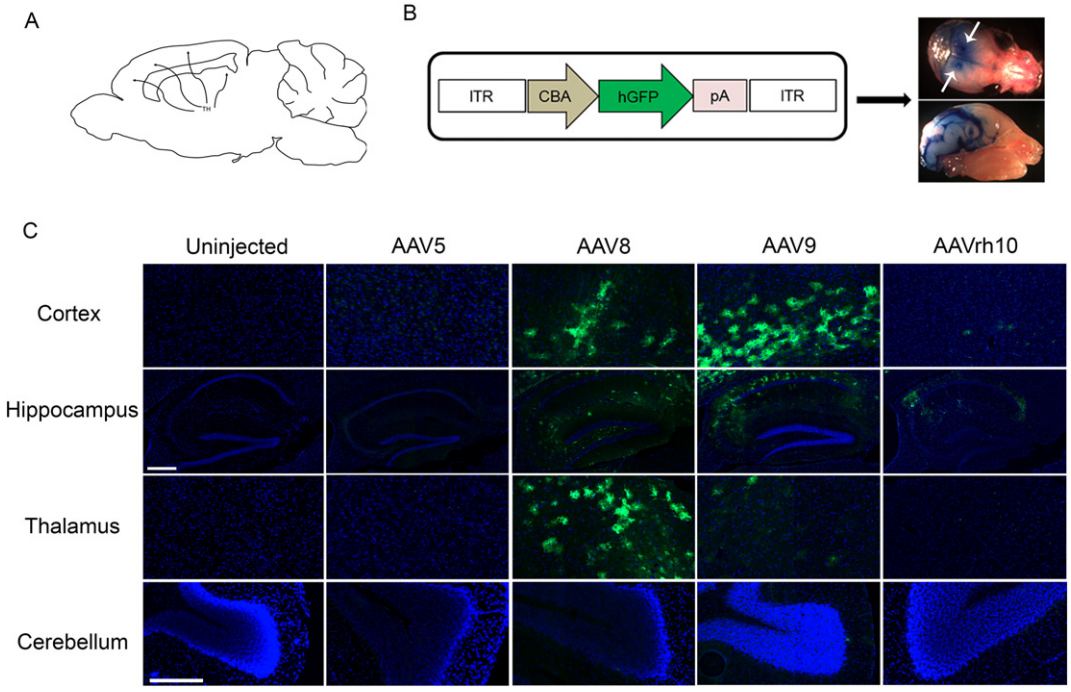


**Fig. 1.** Regional differences in rAAV biodistribution are observed. (A) Representative images showing thalamic connections within the brain (A). Sites of rAAV vector administration into thalamus (white arrows), and predicted rAAV spread within the CNS using 2% Evans Blue dye are shown (B). Representative tissue sections of interest (C) were analyzed for GFP expression in the cortex, hippocampus, thalamus and cerebellum of three month old MPS IIIB animals after rAAV administration. Scale bar: hippocampus (8×), 300 μm; and cortex, thalamus and hippocampus (20×), 100 μm.

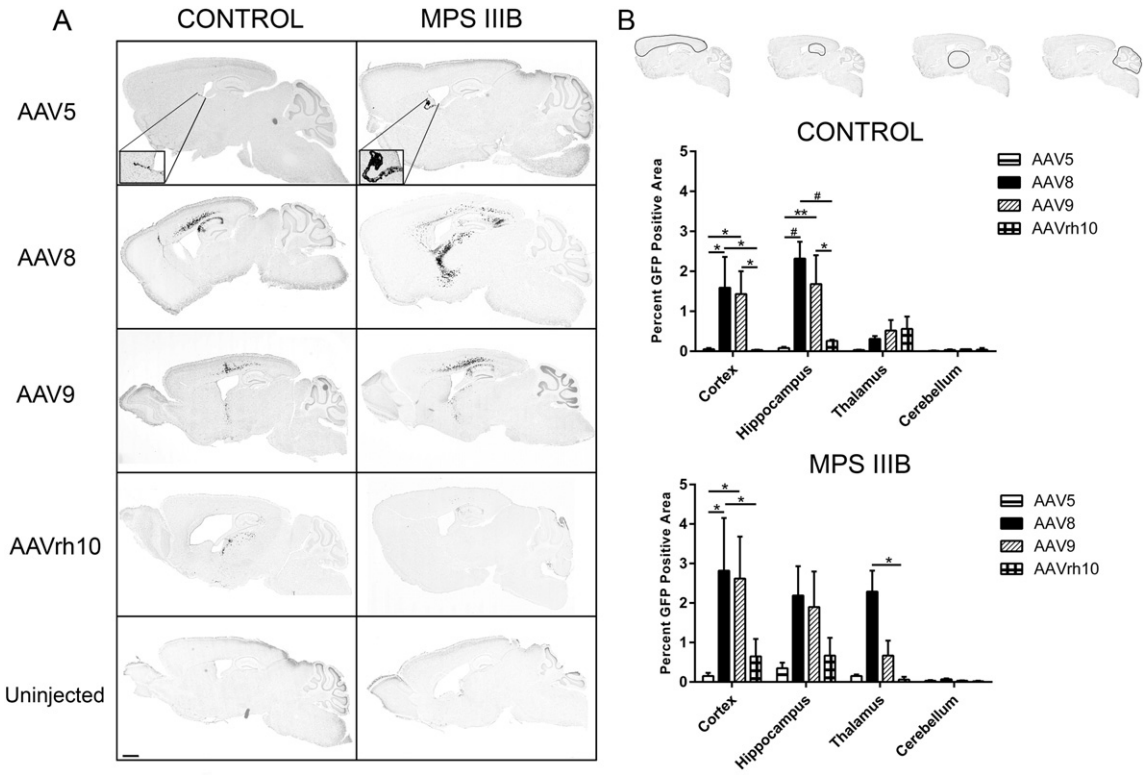


**Fig. 2.** rAAVs exhibit differential biodistributions which may be genotype specific. Mid-sagittal brain sections of Control and MPS IIIB 3 month old littermates were assessed for the presence of AAV–GFP (A, dark areas of grayscale images, scale bar = 2 mm). Inset images depict robust staining of ependymal cells by AAV5. The percentage of regional GFP positive area was then quantitated in the cortex, hippocampus, thalamus and cerebellum (B). All sagittal sections were scanned at 20× magnification and GFP expression was quantified in indicated regions using Aperio ImageScope algorithm. Two-way ANOVA was used to assess differences within region based on serotype, n = 3–4/cohort, $^{*}p < 0.05$; $^{**}p < 0.01$, and $^{\#}p < 0.001$. Data represented as mean ± SEM.

superior to -5 and -rh10 ($p < 0.05$ for both), and in the thalamus, AAV8 was superior to -rh10 ($p < 0.05$). The largest GFP positive area in the thalamus was modulated by AAV8, at approximately 2% (Fig. 2B).

### 2.2. Moderate biodistribution is achieved with thalamic vector administration

As widespread CNS biodistribution is a determinant of therapeutic utility, we sought to assess the degree of biodistribution away from the site of administration. To accomplish this, we selected four spatially distinct, structurally unique, relatively equidistant sagittal sections for quantitative assessment of GFP expression (Fig. 3A). Using the Allen Brain Atlas for reference, the estimated relative anatomical locations, in millimeters, lateral to medial are −4.2, −3.72, −2.72 and −1.72 (Fig. 3B). The GFP positive area of entire tissue sections were quantitated for each of the four sections for both Control (Fig. 3C) and MPS IIIB (Fig. 3D) treated groups. Although no statistical significance was achieved in individual sections for the Control group, a cumulative assessment of all four sections revealed that use of AAV9 resulted in a significantly larger percentage of total GFP positive area than AAV5 and -rh10 ($p < 0.01$ and $p < 0.05$, respectively), but no difference compared to AAV8. In MPS IIIB treated animals, AAV8 resulted in a statistically significant larger percentage of GFP positive area compared to AAVrh10 in Section 1 and both AAV5 and -rh10 in Section 4. Cumulative assessment of all four tissue sections showed that AAV8 was superior to AAV5 and -rh10 ($p < 0.0001$ for both, Fig. 3D), but no difference compared to AAV9. AAV9 also had a larger cumulative transduction area compared to AAV5 ($p < 0.01$) or -rh10 ($p < 0.001$). In other studies, we have observed an increased transduction area with AAV8 in MPS IIIB compared to control animals, which is not seen for the other serotypes tested here. A similar comparison with this study reveals a similar trend that does not reach statistical significance using GFP fluorescence area.

### 2.3. Differential biodistribution of rAAV vectors

To confirm distribution of viral genomes as a correlative assessment to the GFP expression by fluorescence, we performed quantitative PCR of brain regions. One brain hemisphere from each treated animal was dissected into three parts (Fig. 4). Assessment of rAAV genomes present in each of the three tissue segments was determined by qPCR. The “front” includes large structures such as the somatosensory and somatomotor parts of the cortex, caudoputamen and nucleus accumbens. The “middle” includes structures such as the visual areas of the cortex, hippocampus, thalamus, hypothalamus and amygdala and the “back” encompasses the cerebellum and brain stem. As expected, based on injection site, the middle segment contains the largest number of vector genomes, with diminishing returns in the front and back segments, respectively. AAV8 and -9 resulted in the greatest persistence of vector genomes in the middle segment of MPS IIIB treated animals (AAV8 vs -5 and -rh10, $p < 0.0001$ for both, AAV9 vs -5 and -rh10, $p < 0.001$ for both). AAV9 appeared to have higher incorporation of vector genome in the Control group (AAV9 vs -5 and -rh10, $p < 0.01$ and $p < 0.001$, respectively), although overall, fewer vector genomes were incorporated in the Control group. Detection of vector genomes for AAV5 and -rh10 fell below reliable limits of detection in each analyzed section, reflective of the overall minimal expression of GFP observed in tissue sections.

## 3. Discussion

Studies, from several lysosomal storage disease models and from clinical therapies for MPS I and II, suggest that the greatest therapeutic

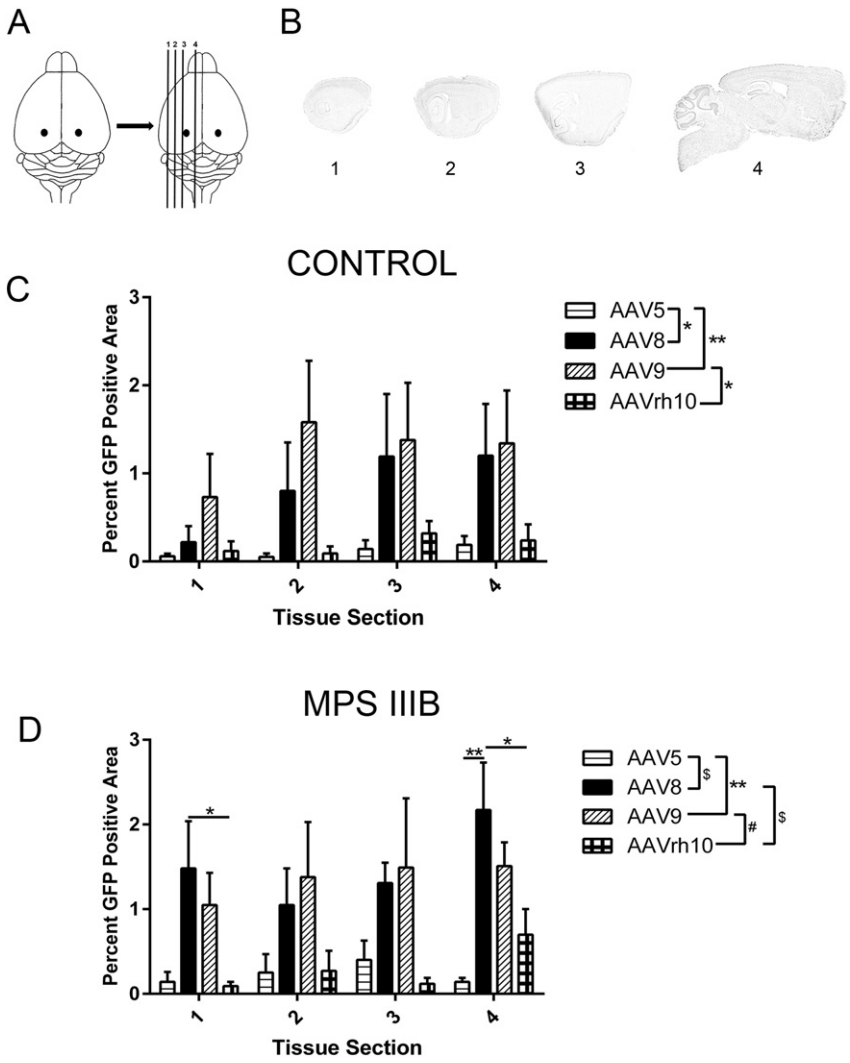


**Fig. 3.** AAV serotype dependent general CNS biodistribution. Three months after rAAV administration, brains are sectioned sagittally (A) into four relatively equidistant sections (B) and collected to assess tissue biodistribution following thalamic infusion. Each tissue section in the Control (C) and MPS IIIB (D) treated groups was analyzed for the presence and percentage of GFP positive area. Two-way ANOVA was used to assess differences within tissue section based on serotype and one-way ANOVA was used to test individual differences between serotype, n = 3–4/cohort, $^{*}p < 0.05$; $^{**}p < 0.01$, $^{\#}p < 0.001$, $^{\$}p < 0.0001$. Data represented as mean ± SEM.

advantage in the treatment of the CNS manifestations associated with MPS IIIB will be garnered when treatment is administered during infancy. Gene therapy continues to be a favored therapeutic approach for the treatment of monogenic diseases such as MPS IIIB. The unique environment of the CNS would facilitate long term therapeutic transgene expression, thereby facilitating disease correction. We have previously demonstrated that a six site intracranial administration of AAV2/5 NAGLU resulted in improvement in brain heparan sulfate storage, hearing, motor coordination and lifespan but did not completely correct the disease [18]. To this end, determination of an optimal AAV vector which both transduces many neuronal cell types and yields high transgene expression; as well as, identification of a minimally invasive, yet highly effective method of delivery remains critical to establishing an efficient therapeutic approach. To address this need, we compared four AAV vector serotypes using the less invasive bilateral thalamic injection method and conducted an analysis of both transduction and biodistribution profiles in the brain. Since each of the four AAV vectors contains identical genetic elements and vector genome concentrations are the same, it is expected that any differences in vector transduction and biodistribution are primarily attributable to the effects of variations in serotype specific capsid amino acid differences on intracellular processing efficiency and respective tropism preferences.

To tease apart differences in AAV vector efficiency and biodistribution as a consequence of thalamic administration, we assessed four areas of functional significance: the cortex, hippocampus, thalamus and cerebellum (Figs. 1 and 2). Interestingly, AAV8 and -9 revealed robust GFP expression in most regions analyzed, while AAV5 and -rh10 were substantially inferior, with overall minimal and faintly expressed GFP. Noteworthy, AAV5 was found predominantly expressed in ependymal cells of the choroid plexus which line the lateral ventricles. This observation was unique to AAV5. This limited tropism suggests the presence of unique cellular properties of ependymal cells, most likely the presence and abundance of N-linked sialic acid receptors [19]. The overall poor distribution of AAV5 suggests unique cell type specific regulation of these receptors, possibly differentially regulated in an age dependent manner. This low distribution is surprising given the efficacy of this vector for disease improvement. The therapeutic efficacy of AAV5 may be accounted for by cross-correction via the mannose-6-phosphate pathway of the NAGLU product secreted and the choroid plexus localization would allow secretion to be distributed into the cerebrospinal fluid to facilitate enzyme distribution. This would not be seen with the current cytoplasmic GFP gene product. Neither the primary nor co-receptor is known for AAVrh10, it is therefore plausible that the presence and abundance of these unknown receptors may be

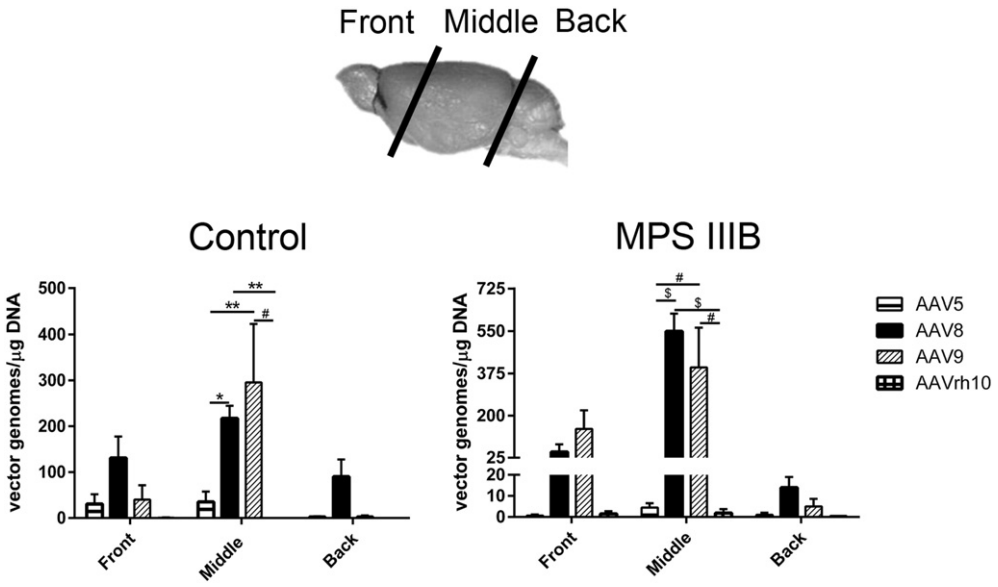


**Fig. 4.** Quantitative PCR for vector genomes in the brain. The right sagittal half of brains from 3 month old control and MPS IIIB mice were dissected into three parts: front, middle and back as shown. The total copies of vector DNA/μg gDNA detected in the CNS of AAV5, -8, -9 and -rh10 treated animals are shown. The positive cutoff limit, ≥100 vg/μg gDNA, is presented by the horizontal trend line. gDNA, genomic DNA. n = 3/cohort, $^{*}p < 0.05$; $^{**}p < 0.01$, $^{\#}p < 0.001$, $^{\$}p < 0.0001$. Data represented as mean ± SEM.

differentially regulated based on extracellular milieu and age. Both AAV5 and -rh10 demonstrated low persistence of vector genomes indicating decreased cell binding and/or increased clearance of the vector. In the control group, statistically significant improvements in GFP biodistribution, modulated by AAV8 and -9, were observed in the cortex and hippocampus. Similarly in the MPS IIIB group, AAV8 and -9 proved superior in the cortex, although no significant differences were observed in the hippocampus. Noteworthy, AAV8 showed more substantial transduction of the thalamic region compared to any other serotype. A qualitative analysis of the AAV8 thalamic transduction pattern in the MPS IIIB group suggests efficient transport along thalamocortical projections and tracks or possible axonal transport, although this was not evident in Control animals. This trend was also evident, but substantially diminished in AAV9 treated Control and MPS IIIB groups, and minimally evident in the -rh10 treated groups. These differential observations suggest serotype specific differential diffusion mechanics. Overall, the maximal GFP positive area of the thalamus was only approximately 2%, and this was mediated by AAV8 in the MPS IIIB group. The variability between control and MPS IIIB brains injected with the different serotypes was large, but the trends were evident. Such serotype dependent variability has been reported by other groups using different models [20–22]. Furthermore, a study of AAV2 injection into the thalamus of GM1 mice showed selective tropism of virus for only a subset of thalamic nuclei. Interestingly, the cerebellum was not efficiently transduced by any serotype, suggesting either a need for delivery of higher AAV titers, larger volume or need for a different method of administration in order to reach this important structure.

To gauge the biodistribution of AAV vectors throughout the brain parenchyma and away from the sites of injection, we quantitated GFP expression on four structurally unique and relatively equidistant tissue sections (Fig. 3). Notable distant GFP expression was observed primarily in AAV8 and -9 treated animals compared to AAV5 and -rh10. Current studies suggest that differential transduction properties of AAVs may be attributed to differences in tropism, receptor usage and availability and perhaps differences in interaction with the extracellular milieu. Nevertheless, the limited CNS transduction does prove problematic. Regardless of serotype, less than 3% of any given tissue area was GFP positive. With the insertion of the therapeutic transgene, whether 3% is sufficient to confer any therapeutic benefit is unclear but presumably a higher level would be preferred. However, we predict that the secretory and diffusive properties of lysosomal enzymes may facilitate cross-correction of neighboring cells and may therefore counteract this limitation [23]. Assessment of vector biodistribution by qPCR revealed that AAV5 and -rh10 fell below reliable levels of detection in each brain section analyzed; whereas, AAV8 and -9 genomes were concentrated predominantly in the middle sections as predicted based on the initial injection areas (Fig. 4). Loss of genomes by AAV5 and -rh10 explain the observed low abundance of GFP expression in previous figures. Although we can't exclude some differences in variation of injection sites, assessment of vector biodistribution, both qualitatively and quantitatively indicate that the abundance of AAV vectors was localized in the 'middle' region of the brain, as indicated in Figs. 1 and 4.

An advantage of using the bilateral thalamic method for vector administration is that it's relatively minimally invasive; however, the inability of AAV vectors to efficiently transduce large brain areas and penetrate parenchyma argues strongly for a different method of administration and limits the utility of this approach. A higher vector titer, possibly administered by convection enhanced delivery (CED), may yield more favorable outcomes [24–26].

## 4. Methods

### 4.1. AAV constructs

Purified stocks of recombinant AAV2 plasmids pseudotyped with capsid proteins from AAV-5, -8, -9 and -rh10 were used in this study, and each contains the hybrid cytomegalovirus enhancer/chicken beta-actin (CMV) promoter driving humanized green fluorescent protein (hGFP) expression. Vectors were produced, and titered at the University of Florida Powell Gene Therapy Center Vector Core Laboratory (Gainesville, FL) as previously described. Briefly, vectors were purified by iodixanol (Sigma, St. Louis, MO) gradient ultracentrifugation followed by ion-exchange chromatography using HiTrap Q HP (GE Healthcare, Piscataway, NJ) and concentrated by centrifugation. Vector titer was determined by dot blot assay as previously described [27]. Briefly, vector DNA was immobilized onto a nylon membrane along with the plasmid standard curve using a dot-blot

apparatus (Bio-Rad, Hercules, CA). The blots are then probed for the transgene. The vector DNA signal was compared to the signal generated via the plasmid DNA standard curve in order to determine a vector genome titer. Titered vectors were aliquoted, diluted and stored at −80 °C for future use.

### 4.2. Mice

The congenic C57BL/6 NAGLU-deficient mouse strain was utilized and expanded by strict sibling mating [3]. Genotyping was done on tissue of postnatal day 2 pups by enzyme assay or NAGLU exon 6 and neomycin insertion cassette PCR [28]. Phenotypically indistinguishable wild type (+/+) and heterozygous (−/+) (subsequently referred to as "Control") and mutant (−/−) MPS IIIB mice were identified and allocated for further study. All animal studies were performed in accordance with the guidelines of the University of Florida Institutional Animal Care and Use Committee.

### 4.3. Treatments

All rAAV vector injections were performed in mouse pups at 3–4 days of age. For vector administration, genotyped pups were cryoanesthetized prior to bilateral thalamic infusion. Each pup received a total of $4.8 \times 10$ [9] vector genomes administered in 2 μl per site using a 32-gauge Hamilton syringe (Narishige Int., East Meadow, NY). Injection coordinates were (from bregma: 4 mm posterior, 1 mm lateral and 3 mm deep). For each rAAV serotype, 3 control and 3–4 MPS IIIB neonatal mice were injected. Prior to injections, neonatal animals were immobilized by cryoanesthetization. All treatment was well tolerated and animals were warmed until movement returned prior to being returned to their mothers.

### 4.4. Histological procedures

Animals were sacrificed three months after vector infusion. Mice were euthanized with 100 μl of ketamine (120 mg/kg)/xylazine (16 mg/kg) cocktail followed by thoracotomy. Transcardial perfusion with 1 × PBS followed by fresh ice-cold 4% paraformaldehyde in 1 × PBS solution followed. Brains were harvested and post-fixed for 3 h in 4% paraformaldehyde at 4 °C, followed by overnight incubation in 20% sucrose in 1 × PBS at 4 °C. One brain hemisphere was then embedded in O.C.T (Triangle Biomedical Sciences, Durham, NC) and rapidly frozen in a 2-methyl-butane/dry ice bath. Sagittal sections were cut to a thickness of 20 μm and stored in a cryoprotective solution at −80 °C until use.

### 4.5. Quantitation of GFP

To assess total GFP positive area, automated whole-section imaging of brain tissue was conducted using the Scanscope FL instrument (Aperio Technologies, Vista, CA). The Positive Pixel Count FL v1 algorithm within ImageScope was used for quantitation of GFP within delineated areas of brain tissue. Again, the Allen Reference Atlas (ARA) was used as a neuroanatomical reference. GFP positive area was determined using the average from three independent tests performed by three readers in a blinded manner. The minimum GFP intensity was set between 0.2 and 0.4, while the maximum intensity was set to 1.

### 4.6. Vector copy number determination

Total genomic DNA was isolated from brain tissue using a standard phenol:chloroform:isoamyl protocol. AAV vector genome copy numbers were determined by qPCR using Life Technologies Universal SYBR Green Mastermix (Bio-Rad Laboratories, Hercules, CA). Total DNA concentration was determined by spectrophotometry using NanoDrop (Thermo Scientific, Ashville, NC). Vector genomes were quantitated using primers targeting GFP; forward: 5′-TCGCCGATTGGAGTGTTCTG TTG-3′ and reverse: 3′-ATGGAAACATTCTCGGCCACAAGC-5′. Known copy numbers of a plasmid containing the GFP gene were used to construct the standard curve. Results are expressed as the number of vector copy numbers per μg of genomic DNA. The positive cutoff limit was set to ≥100 vg/μg gDNA.

### 4.7. Statistical analysis

GraphPad Prism 6 was used for statistical analysis. One-way ANOVA with Bonferroni post-test corrections and two-way ANOVA with Tukey's post-test corrections were used for multiple comparisons. Student's t-test was used for unpaired data. Bar graphs are shown as mean ± SEM. Probability $p < 0.05$ was considered statistically significant.

## Acknowledgements

This work was supported by the Gatorade Trust through funds distributed by the University of Florida, Department of Medicine and by NIH-NIDDK K085141-01 (CDH).

## References

[1] G. Yogalingam, J.J. Hopwood, Molecular genetics of mucopolysaccharidosis type IIIA and IIIB: diagnostic, clinical, and biological implications, Hum. Mutat. 18 (2001) 264–281.
[2] J.A. Gilkes, C.D. Heldermon, Mucopolysaccharidosis III (Sanfilippo syndrome) — disease presentation and experimental therapies, Pediatr. Endocrinol. Rev. 12 (Suppl. 1) (2014) 133–140.
[3] H.H. Li, et al., Mouse model of Sanfilippo syndrome type B produced by targeted disruption of the gene encoding ?-N-acetylglucosaminidase, Proc. Natl. Acad. Sci. U. S. A. 96 (1999) 14505–14510.
[4] C.D. Heldermon, et al., Development of sensory, motor and behavioral deficits in the murine model of Sanfilippo Syndrome Type B, PLoS One 2 (2007), e772.
[5] T.R. Flotte, Gene therapy progress and prospects: recombinant adeno-associated virus (rAAV) vectors, Gene Ther. 11 (2004) 805–810.
[6] M.G. Kaplitt, et al., Long-term gene expression and phenotypic correction using adeno-associated virus vectors in the mammalian brain, Nat. Genet. 8 (1994) 148–154.
[7] F. Mingozzi, K.A. High, Therapeutic in vivo gene transfer for genetic disease using AAV: progress and challenges, Nat Rev Genet 12 (2011) 341–355.
[8] J.E. Rabinowitz, et al., Cross-packaging of a single adeno-associated virus (AAV) type 2 vector genome into multiple AAV serotypes enables transduction with broad specificity, J. Virol. 76 (2002) 791–801.
[9] G. Gao, et al., Clades of adeno-associated viruses are widely disseminated in human tissues, J. Virol. 78 (2004) 6381–6388.
[10] J.E. Rabinowitz, et al., Cross-dressing the virion: the transcapsidation of adeno-associated virus serotypes functionally defines subgroups, J. Virol. 78 (2004) 4421–4432.
[11] C. Burger, et al., Recombinant AAV viral vectors pseudotyped with viral capsids from serotypes 1, 2, and 5 display differential efficiency and cell tropism after delivery to different regions of the central nervous system, Mol. Ther. 10 (2004) 302–317.
[12] J.-M. Taymans, et al., Comparative analysis of adeno-associated viral vector serotypes 1, 2, 5, 7, and 8 in mouse brain, Hum. Gene Ther. 18 (2007) 195–206.
[13] P. Chakrabarty, et al., Capsid serotype and timing of injection determines AAV transduction in the neonatal mice brain, PLoS One 8 (2013), e67680.
[14] T.M. Daly, C. Vogler, B. Levy, M.E. Haskins, M.S. Sands, Neonatal gene transfer leads to widespread correction of pathology in a murine model of lysosomal storage disease, Proc. Natl. Acad. Sci. U. S. A. 96 (1999) 2296–2300.
[15] M.L.D. Broekman, L.A. Comer, B.T. Hyman, M. Sena-Esteves, Adeno-associated virus vectors serotyped with AAV8 capsid are more efficient than AAV-1 or -2 serotypes for widespread gene delivery to the neonatal mouse brain, Neuroscience 138 (2006) 501–510.
[16] B.L. Gliddon, J.J. Hopwood, Enzyme-replacement therapy from birth delays the development of behavior and learning problems in mucopolysaccharidosis type IIIA mice, Pediatr. Res. 56 (2004) 65–72.
[17] C.D. Heldermon, et al., Disease correction by combined neonatal intracranial AAV and systemic lentiviral gene therapy in Sanfilippo Syndrome type B mice, Gene Ther. 20 (2013) 913–921.
[18] C.D. Heldermon, et al., Therapeutic efficacy of bone marrow transplant, intracranial AAV-mediated gene therapy, or both in the mouse model of MPS IIIB, Mol. Ther. 18 (2010) 873–880.
[19] M. Nonnenmacher, T. Weber, Intracellular transport of recombinant adeno-associated virus vectors, Gene Ther. 19 (2012) 649–658.
[20] C.N. Cearley, J.H. Wolfe, Transduction characteristics of adeno-associated virus vectors expressing cap serotypes 7, 8, 9, and Rh10 in the mouse brain, Mol. Ther. 13 (2006) 528–537.
[21] R. Holehonnur, et al., Adeno-associated viral serotypes produce differing titers and differentially transduce neurons within the rat basal and lateral amygdala, BMC Neurosci. 15 (2014) 28.
[22] B.L. Davidson, et al., Recombinant adeno-associated virus type 2, 4, and 5 vectors: transduction of variant cell types and regions in the mammalian central nervous system, Proc. Natl. Acad. Sci. 97 (2000) 3428–3432.
[23] A.F. Skorupa, K.J. Fisher, J.M. Wilson, M.K. Parente, J.H. Wolfe, Sustained production of beta-glucuronidase from localized sites after AAV vector gene transfer results in widespread distribution of enzyme and reversal of lysosomal storage lesions in a large volume of brain in mucopolysaccharidosis VII mice, Exp. Neurol. 160 (1999) 17–27.

[24] N.U. Barua, et al., Convection-enhanced delivery of AAV2 in white matter—a novel method for gene delivery to cerebral cortex, J. Neurosci. Methods 220 (2013) 1–8.
[25] A.P. Kells, et al., Efficient gene therapy-based method for the delivery of therapeutics to primate cortex, PNAS 106 (2009) 2407–2411.
[26] N. Carty, et al., Convection-enhanced delivery and systemic mannitol increase gene product distribution of AAV vectors 5, 8, and 9 and increase gene product in the adult mouse brain, J. Neurosci. Methods 194 (2010) 144–153.
[27] S. Zolotukhin, et al., Production and purification of serotype 1, 2, and 5 recombinant adeno-associated viral vectors, Methods 28 (2002) 158–167.
[28] J. Marsh, A.H. Fensom, 4-Methylumbelliferyl alpha-N-acetylglucosaminidase activity for diagnosis of Sanfilippo B disease, Clin. Genet. 27 (1985) 258–262.